nature medicine

Alternatively activated macrophages do not synthesize catecholamines or contribute to adipose tissue adaptive thermogenesis

Katrin Fischer[1,2], Henry H Ruiz[3], Kevin Jhun[3], Brian Finan[1,2], Douglas J Oberlin[3], Verena van der Heide[3], Anastasia V Kalinovich[4], Natasa Petrovic[4], Yochai Wolf[5], Christoffer Clemmensen[1,2], Andrew C Shin[3,13], Senad Divanovic[6], Frank Brombacher[7], Elke Glasmacher[1], Susanne Keipert[1], Martin Jastroch[1,8], Joachim Nagler[9], Karl-Werner Schramm[9], Dasa Medrikova[10], Gustav Collden[1,2], Stephen C Woods[11], Stephan Herzig[10], Dirk Homann[3], Steffen Jung[5], Jan Nedergaard[4], Barbara Cannon[4], Matthias H Tschöp[1,2], Timo D Müller[1,14] & Christoph Buettner[3,12,14]

Adaptive thermogenesis is the process of heat generation in response to cold stimulation. It is under the control of the sympathetic nervous system, whose chief effector is the catecholamine norepinephrine (NE). NE enhances thermogenesis through β3-adrenergic receptors to activate brown adipose tissue and by 'browning' white adipose tissue. Recent studies have reported that alternative activation of macrophages in response to interleukin (IL)-4 stimulation induces the expression of tyrosine hydroxylase (TH), a key enzyme in the catecholamine synthesis pathway, and that this activation provides an alternative source of locally produced catecholamines during the thermogenic process. Here we report that the deletion of *Th* in hematopoietic cells of adult mice neither alters energy expenditure upon cold exposure nor reduces browning in inguinal adipose tissue. Bone marrow–derived macrophages did not release NE in response to stimulation with IL-4, and conditioned media from IL-4-stimulated macrophages failed to induce expression of thermogenic genes, such as uncoupling protein 1 (*Ucp1*), in adipocytes cultured with the conditioned media. Furthermore, chronic treatment with IL-4 failed to increase energy expenditure in wild-type, *Ucp1*$^{-/-}$ and interleukin-4 receptor-α double-negative (*Il4ra*$^{-/-}$) mice. In agreement with these findings, adipose-tissue-resident macrophages did not express TH. Thus, we conclude that alternatively activated macrophages do not synthesize relevant amounts of catecholamines, and hence, are not likely to have a direct role in adipocyte metabolism or adaptive thermogenesis.

Thermogenesis is crucial for the survival of endothermic mammals and birds because it enables the organism to maintain a stable body temperature even in a cold environment[1,2]. Hypothermia has been a major cause of mortality for these animals throughout their evolutionary history. Consequently, the need for efficient thermogenesis represents an evolutionary pressure that has shaped the biology of all endothermic homeotherms[3]. Thermogenesis also plays a central part in energy homeostasis, and pharmacological stimulation of energy expenditure is considered to be a valuable strategy for combatting obesity and its comorbidities[4]. A detailed understanding of the physiological and molecular underpinnings that regulate adaptive thermogenesis is therefore of utmost importance. It is well established that catecholamines are a key driver of thermogenesis, which they induce by stimulating uncoupled respiration in brown adipose tissue (BAT) and beige, or 'brite' (beige/brite), white adipose tissue (WAT). Notably, catecholamines are also key for the induction of lipolysis in WAT that prompts the release of fatty acids, the principal substrates for BAT thermogenesis[5]. In the periphery, catecholamines have classically been thought to originate from either sympathetic postganglionic neurons or, otherwise, the adrenal medulla. Challenging this conventional

[1]Institute for Diabetes and Obesity, Helmholtz Diabetes Center (HDC), Helmholtz Zentrum München and German Center for Diabetes Research (DZD), München-Neuherberg, Germany. [2]Division of Metabolic Diseases, Department of Medicine, Technische Universität München, Munich, Germany. [3]Diabetes, Metabolism and Obesity Institute, Icahn School of Medicine at Mount Sinai, New York, New York, USA. [4]Department of Molecular Biosciences, The Wenner-Gren Institute, Stockholm University, Stockholm, Sweden. [5]Weizmann Institute of Science Department of Immunology, Rehovot, Israel. [6]Department of Pediatrics, Division of Immunobiology, Cincinnati Children's Hospital Medical Center, Cincinnati, Ohio, USA. [7]International Center for Genetic Engineering and Biotechnology, Cape Town component & University of Cape Town, IDM, Division Immunology & SAMRC, Cape Town, South Africa. [8]Department of Animal Physiology, Faculty of Biology, Philipps University of Marburg, Marburg, Germany. [9]Molecular Exposomics, Helmholtz Zentrum München, German National Diabetes Center (DZD), Neuherberg, Germany. [10]Institute for Diabetes and Cancer (IDC), Helmholtz Zentrum München, German National Diabetes Center (DZD), Neuherberg, Germany, and Joint IDC-Heidelberg Translational Diabetes Program, Inner Medicine I, Heidelberg University Hospital, Heidelberg, Germany. [11]Metabolic Diseases Institute, Department of Psychiatry and Behavioral Neuroscience, University of Cincinnati, Cincinnati, Ohio, USA. [12]Department of Medicine, Icahn School of Medicine at Mount Sinai, New York, New York, USA. [13]Present address: Department of Nutritional Sciences, College of Human Sciences, Texas Tech University, Lubbock, Texas, USA. [14]These authors contributed equally to this work. Correspondence should be addressed to T.D.M. (timo.mueller@helmholtz-muenchen.de) or C.B. (christoph.buettner@mssm.edu).

Received 10 November 2016; accepted 6 March 2017; published online 17 April 2017; doi:10.1038/nm.4316

view, recent reports have proposed a major paradigm shift by suggesting that alternatively activated macrophages are another important source of catecholamines, and that they consequently represent a previously overlooked mechanism behind the regulation of thermogenesis. In such a model, cold exposure enhances alternative activation of macrophages, which thereby induces TH enzyme, which in turn results in the production and secretion of NE to enhance nonshivering thermogenesis in BAT, lipolysis in WAT[6] and browning of inguinal WAT (iWAT)[7]. Most of the data on which this concept rests are derived from *in vivo* experiments that analyzed mice with a lifelong deficiency of key 'M2 signaling nodes', i.e., mice systemically deficient in *Il4*/*13*, *Il4ra* or *Stat6*, and mice with myeloid-cell-specific deletion of *Il4ra* and *Th*. Notably, all of these germline-knockout (KO) models share the caveat that their metabolic phenotypes can be compromised through developmental processes and/or through altered sympathetic regulation because all of these genes are also expressed in the central nervous system (CNS). Accordingly, the aim of the present studies was to assess the role of macrophages in mice with adult-onset peripheral deletion of *Th*, as well as to further evaluate the role of alternatively activated macrophages in the regulation of white, brown and beige/brite adipocyte function *in vitro* and *in vivo*. Collectively, we show here, using a combination of *in vivo* and *in vitro* approaches, that alternatively activated macrophages do not synthesize sufficient amounts of catecholamines and are thus unlikely to have a direct role in adipocyte metabolism or adaptive thermogenesis.

RESULTS

Peripheral catecholamines control thermogenesis

Lifelong deletion of *Th* results in early embryonic lethality, possibly owing to the important role of catecholamines in the CNS during development[8]. To study the role of peripheral catecholamines in thermoregulation, we generated mice, herein called THΔper mice, in which *Th* can be inducibly deleted in all peripheral tissues of adult mice, including the sympathetic nervous system (SNS) and hematological cells, but not the CNS. This was accomplished by crossing a strain of mice in which Cre expression is under the control of the *Rosa26* locus that is induced upon tamoxifen administration with a mouse harboring floxed alleles of *Th*, and owing to poor Cre expression in the CNS, the deletion of the *Th* allele does not occur in the CNS (**Fig. 1a**). Ablation of the TH protein in peripheral tissues (BAT, spleen, liver and epididymal white adipose tissue (eWAT)) after tamoxifen administration in adult mice was confirmed by western blot analysis (**Fig. 1b**), and this resulted in marked depletion of NE levels in all peripheral tissues analyzed, as compared to wild-type (WT) controls (**Fig. 1c**). In line with the prediction that THΔper mice have reduced sympathetic activity relative to WT controls, the animals exhibited impaired thermoregulation when exposed to 4 °C (**Fig. 1d**), which is consistent with a key role of catecholamines in thermogenesis. We also used tissue extracts from these mice to validate several commercially available antibodies against TH, several of which had a strong, nonspecific band of similar molecular size as TH, which raises the concern that, without appropriate controls, it might be difficult to ascertain the specificity of any of these antibodies in applications such as western blot (**Supplementary Fig. 1**).

To probe whether catecholamines produced by alternatively activated macrophages play an appreciable part in thermoregulation, we generated bone marrow–chimeric mice, in which *Th* is specifically deleted from hematopoietic cells (including macrophages) in an inducible manner. We first transplanted bone marrow from WT and noninduced THΔper mice into irradiated WT recipient mice.

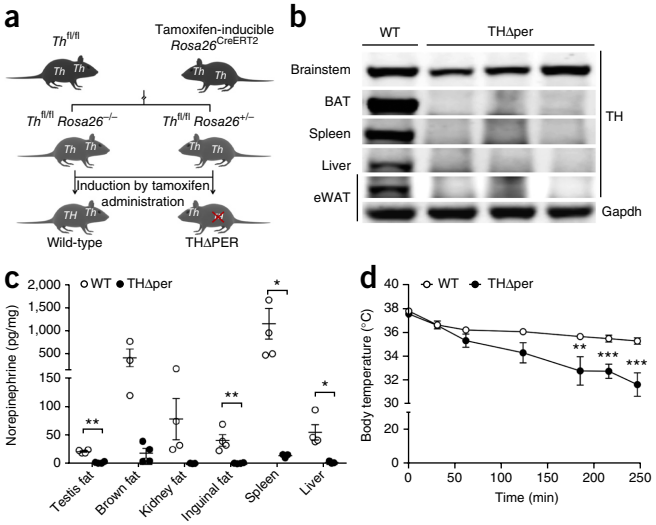

Figure 1 Selective deletion of *Th* in peripheral but not CNS tissues results in peripheral catecholamine depletion and impaired thermoregulation. (**a**) Schematic of the inducible peripheral *Th* knockout (THΔper) mouse model. (**b**) Representative western blot images of indicated tissues from WT or THΔper mice. Uncropped western blot images are shown in **Supplementary Figure 11**. For WT and THΔper mice, $n = 2$ and $n = 3$ samples (brainstem), $n = 7$ and $n = 5$ (BAT), $n = 4$ and $n = 6$ (spleen), $n = 4$ and $n = 4$ (liver) and $n = 1$ and $n = 3$ (eWAT). Gapdh of eWAT was chosen as a representative image for the loading control; comparable Gapdh loading for other tissues is shown in **Supplementary Figure 11**. (**c**) The level of norepinephrine in peripheral tissues of WT ($n = 3$–5) and THΔper ($n = 3$ or 4) mice; each dot represents one animal. (**d**) Body temperature of WT ($n = 7$) and THΔper mice ($n = 7$) during a cold-tolerance test at 4 °C. Data represent mean ± s.e.m. $^*P < 0.05$; $^{**}P < 0.01$; $^{***}P < 0.001$ according to a two-sided Student's *t*-test (**c**) or two-way analysis of variance (ANOVA) followed by a Bonferroni *post hoc* comparison of the individual time points (**d**).

Fluorescence-activated cell sorting (FACS) analysis conducted on peripheral blood ~8 weeks later revealed a >90% reconstitution with lymphocytes and granulocytes of WT or THΔper donor origin in the majority of chimeras (**Fig. 2a**). Subsequent tamoxifen treatment of the chimeras resulted in *Th* ablation from hematopoietic cells (including macrophages) in THΔper, but not WT, chimeras without affecting body weight (**Fig. 2b**). Notably, energy expenditure did not differ between THΔper chimeric mice and their WT controls at room temperature (21 °C) and after exposure to cold at successively lower temperatures of 15 °C, 10 °C and 6 °C (**Fig. 2c**,**d**). Furthermore, locomotor activity (**Fig. 2e**), substrate utilization—as assessed by the respiratory exchange ratio (RER) (**Fig. 2f**)—and core body temperature (**Fig. 2g**) were not different between the mouse types. In keeping with the observation that energy expenditure and core body temperature were not changed after *Th* deletion in hematologic cells, THΔper chimera also exhibited a cold-induced increase in iWAT *Ucp1* mRNA levels comparable to that seen in WT controls (**Fig. 2h**).

No role of macrophages in browning of white adipocytes

To evaluate a possible role of macrophages in adipocyte metabolism *in vitro*, we isolated preadipocytes from iWAT, depleted the macrophages by magnetic-bead-mediated sorting of CD11b-positive cells and cultured and differentiated them *in vitro* (henceforth described as 'primary cells'). We confirmed successful macrophage depletion by the lack of the integrin subunit alpha M (*Itgam*, also known as *Cd11b*) and the adhesion G-protein-coupled receptor E1 (*Adgre1*) mRNA levels

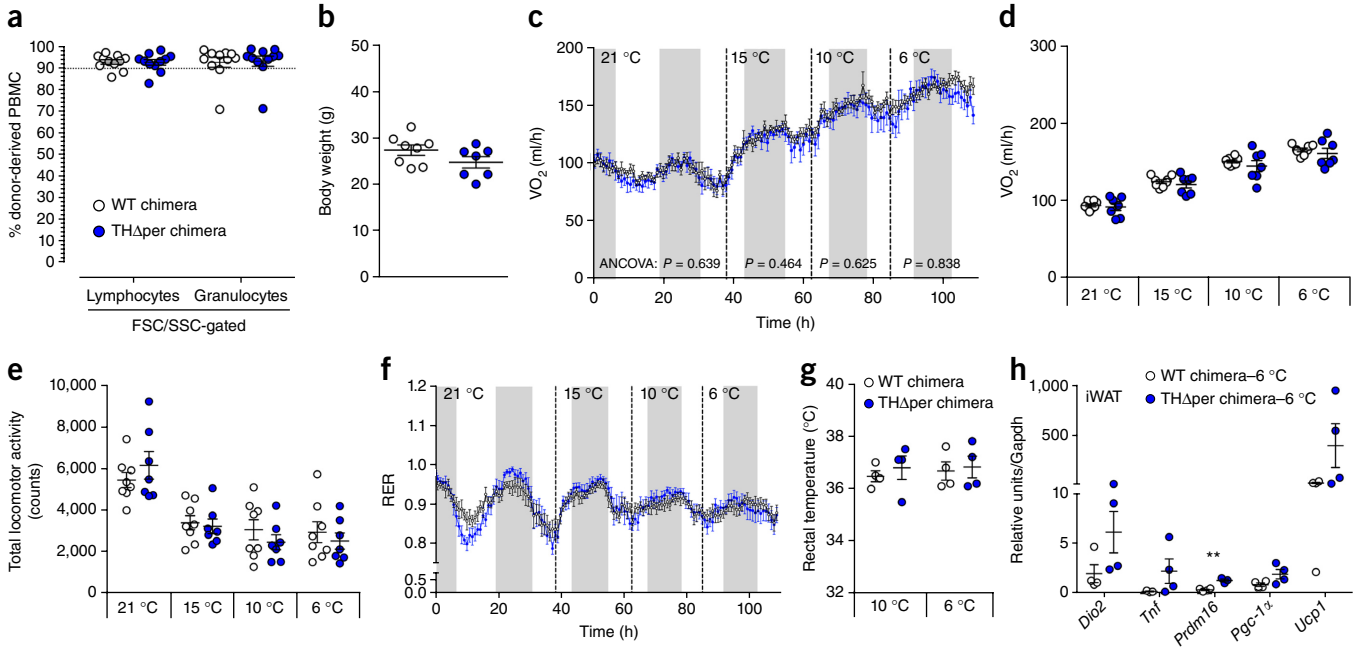

Figure 2 Energy expenditure of WT and THΔper chimera. (**a**) Percentage of donor-derived hematopoietic cells in peripheral blood 8 weeks after BM transplantation from WT ($n = 11$) or THΔper mice into WT mice ($n = 11$), designated from here on as WT chimera and THΔper chimera (FSC, forward scatter; SSC, sided scatter; dashed line indicates acceptable donor reconstitution above 90%). (**b**) Body weight of chimera. (**c**–**f**) Energy expenditure as determined by longitudinal (**c**) and average (**d**) oxygen consumption rate, total locomotor activity (**e**) and RER (**f**) during a successive reduction in ambient temperatures (21, 15, 10 or 6 °C) ($n = 8$ WT and $n = 7$ THΔper chimera). (**g**) Rectal temperature of WT ($n = 4$) and THΔper chimera ($n = 4$), exposed to either 10 °C or 6 °C for 24 h. (**h**) Gene expression of browning and brown-fat thermogenesis markers (*Dio2*, *Tnf*, *Prdm16*, *Pgc-1α* and *Ucp1*) in iWAT from WT ($n = 4$) and THΔper chimera ($n = 4$) after 24 h of exposure to 6 °C. Data represent means ± s.e.m. $^*P < 0.05$; $^{**}P < 0.01$ according to a two-sided Student's *t*-test (**a**,**b**,**d**,**e**,**g**,**h**), analysis of covariance (ANCOVA) with body weight as covariate (**c**), or two-way ANOVA followed by Bonferroni *post hoc* comparison (**f**).

during adipocyte differentiation (**Supplementary Fig. 2a**,**b**) and absence of M1 and M2 markers (*Tnf, Arg1, Mgl2, Mrc1* and *Il10*) in fully differentiated iWAT primary cells (**Supplementary Fig. 2c**,**d**). Lipid accumulation, as assessed by Oil Red O staining, was not affected by the absence of macrophages (**Supplementary Fig. 2e**,**f**), which indicates that macrophages are dispensable for adipocyte differentiation. Consistent with this notion, the expression profiles of markers indicative of adipocyte differentiation (*Fasn*, *Adipoq*, *Fabp4* and *Pparg*) were not affected by the absence of macrophages (**Supplementary Fig. 2g**–**j**). Similarly, we observed no changes for gene programs indicative of fatty acid synthesis, fatty acid transport, cytokine signaling, lipoprotein metabolism, carbohydrate metabolism, lipogenesis or lipolysis (**Supplementary Fig. 2k**–**p**). Furthermore, we observed no differences in the expression profiles of genes related to mitochondrial electron transport (*Cycs* and *Cox4i1*) (**Supplementary Fig. 3a**,**b**) or of key thermogenic genes (*Ucp1, Ppargc1a* (also known as *Pgc-1α*) and *Prdm16*) during the differentiation of iWAT primary cells (**Supplementary Fig. 3c**–**e**).

We next asked whether the depletion of macrophages impaired the ability of isoproterenol to stimulate the expression of *Ucp1* and *Pgc-1α* in differentiated iWAT primary cells and found no difference between the WT cells and those devoid of macrophages (**Supplementary Fig. 3f**,**g**). Consistent with the observation that isoproterenol-induced stimulation of *Ucp1* and *Pgc-1α* is not affected by the absence of macrophages, we observed no changes in basal respiration, ATP production, maximal respiration or nonmitochondrial respiration, as assessed by the oxygen consumption rate (OCR), following treatment with isoproterenol, oligomycin, carbonyl cyanide-4-(trifluoromethoxy)phenylhydrazone (FCCP) or rotenone/antimycin A/2-deoxyglucose (**Supplementary Fig. 3h**–**j**).

To test whether macrophages first need to undergo polarization to stimulate thermogenesis, we treated bone marrow–derived macrophages (BMDMs) with various doses of IL-4 (5 ng/ml, 10 ng/ml or 20 ng/ml) and then used the conditioned media (CM) to stimulate differentiated iWAT primary cells. IL-4 treatment robustly enhanced expression of the M2 markers *Arg1*, *Mrc1* and *Mgl2* in the BMDMs, as compared to vehicle treatment (**Fig. 3a**–**c**). However, despite robust polarization, the CM failed to stimulate the expression of *Ucp1* or *Pgc-1α* in the differentiated iWAT primary cells, indicating that the M2-polarized BMDMs fail to sufficiently secrete NE into media (**Fig. 3d**,**e**). In summary, these data suggest that macrophages are neither required for the differentiation of iWAT primary adipocytes, nor likely to play a part in browning or β-adrenergic-receptor-mediated stimulation of thermogenesis in these cells.

M2 macrophages do not affect thermogenesis in BAT primary cells

To evaluate the thermogenic effect of M2-activated macrophages in BAT, we used CM from IL-4-stimulated BMDMs (IL-4-CM) to stimulate differentiated BAT primary cells. Despite robust M2 polarization of the BMDMs (**Fig. 3a**–**c**), we observed no effect of the CM on the expression of *Ucp1* and *Pgc-1α* (**Fig. 3f**,**g**), which is congruent with the findings obtained in iWAT primary cells (**Fig. 3d**,**e**). IL-4-CM also failed to activate hormone-sensitive lipase (HSL) at all IL-4 doses tested (**Fig. 3h**,**i**) and independently of the duration of IL-4 treatment (15 min, 1 h, 3 h or 6 h) (**Supplementary Fig. 4**). Notably, we confirmed the failure of M2 macrophages to induce thermogenic gene programs in iWAT and BAT primary cells in several independent experiments, which were carried out in primary cells obtained from

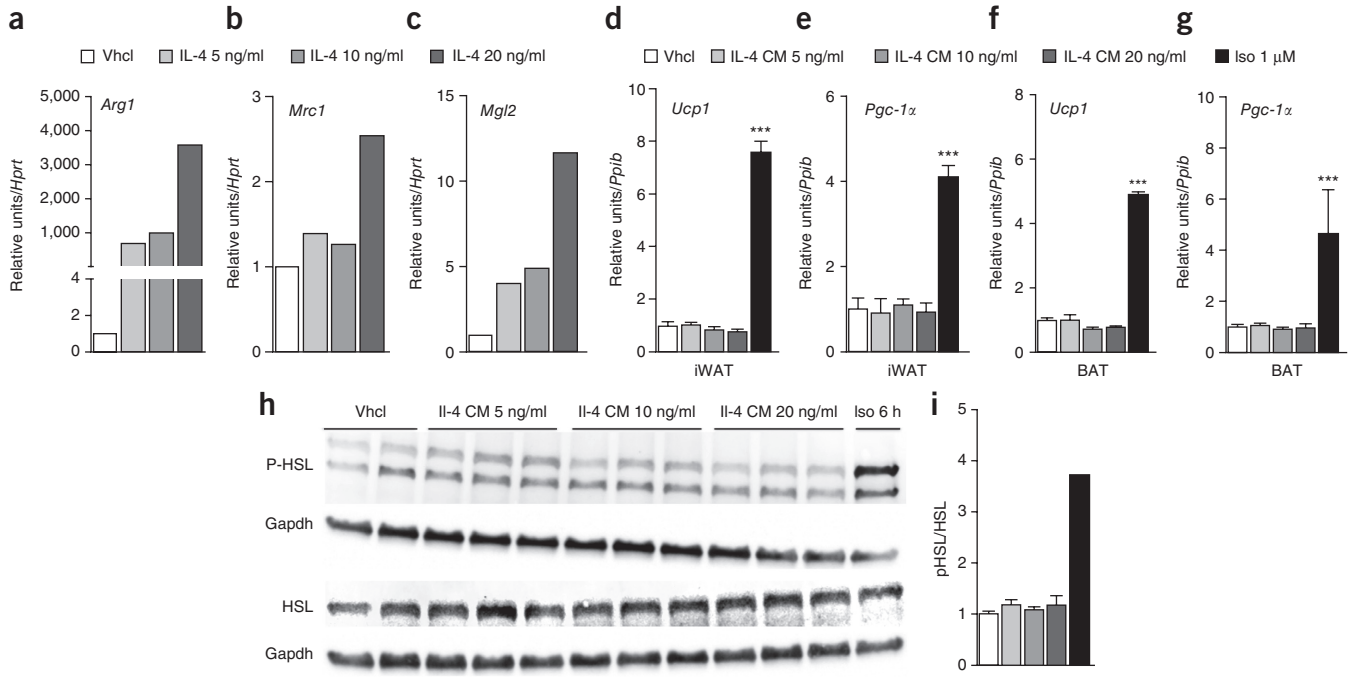

Figure 3 Effect of alternatively activated macrophages from BALB/c mice on thermogenesis in primary inguinal white and brown adipocytes. (**a**–**c**) Representative expression profile of M2 macrophage markers (*Arg1, Mrc1* and *Mgl2*), normalized to hypoxanthine guanine phosphoribosyl transferase (*Hprt*), in IL-4-treated BMDM cells (graphs show one out of three independently performed experiments). (**d**–**g**) Gene expression of brown-fat-specific markers (*Ucp1* and *Pgc-1α*), normalized to peptidylprolyl isomerase B (*Ppib*), in conditioned media from IL-4-treated BMDMs (IL-4-CM) or isoproterenol (Iso)-treated iWAT (**d**,**e**) or BAT (**f**,**g**) primary cells for 6 h. Displayed results are representative of three independently performed experiments, each performed with $n = 3$ technical replicates. (**h**,**i**) Representative western blot (**h**) and quantification (**i**) of phosphorylated or total HSL of 6-d differentiated BAT primary cells treated with IL-4-CM or Iso (1 µM) for 6 h. Western blot in **h** shows one out of three independently performed experiments, each performed with $n = 3$ technical replicates. Uncropped western blot images are shown in **Supplementary Figure 11**. Data represent means ± s.e.m. $^{*}P < 0.05$; $^{**}P < 0.01$; $^{***}P < 0.001$ on the basis of a one-way ANOVA followed by Bonferroni multiple-comparison test.

both BALB/c (**Fig. 3**) and C57BL/6J mice (data not shown), and also from primary cells stimulated with IL-4-CM from Raw264.7 cells (**Supplementary Fig. 5**).

The failure of IL-4-CM to stimulate thermogenic gene programs in both iWAT and BAT primary cells prompted us to quantify IL-4-stimulated catecholamine production in BMDMs. Notably, despite robust IL-4 induction of M2 polarization (**Fig. 3a**–**c**), high-performance liquid chromatography (HPLC) analysis revealed no stimulatory effect of IL-4 relative to vehicle control at any tested dose (5, 10 or 20 ng/ml) on NE, epinephrine, 5-hydroxyindoleacetic acid, homovanillic acid, dopamine or 5-hydroxytryptamin (**Supplementary Fig. 6**). Of note, IL-4 failed to induce catecholamine levels in both the supernatant (**Supplementary Fig. 6a**–**f**) and in the macrophages themselves (**Supplementary Fig. 6g**–**l**). These data suggest that M2 macrophages lack the ability to produce sufficient catecholamines and thus to induce thermogenic gene programs in iWAT or BAT primary cells.

Chronic IL-4 treatment has no effect on energy metabolism

We next assessed whether chronic IL-4 treatment in WT and *Il4ra*$^{-/-}$ mice exposed to various declining environmental temperatures (30 °C, 20 °C, 10 °C or 5 °C) alters energy expenditure. Daily intraperitoneal administration of IL-4 (50 µg/kg) for 12 d did not alter body weight (**Fig. 4a**) or energy expenditure in WT or *Il4ra*$^{-/-}$ mice at any temperature tested (**Fig. 4b**,**c**). Notably, despite robust induction of M2 polarization in the BAT (**Fig. 4d**–**f**) after IL-4 treatment—confirming that the IL-4 was fully functional—such treatment did not increase the expression of *Ucp1* or *Pgc-1α* in BAT relative to controls (**Fig. 4g**,**h**). Mice lacking *Il4ra* show no elevated expression of *Arg1*, *Mrc1* or *Mgl2* after IL-4 treatment (**Fig. 4d**–**f**), which thus confirms their inability to activate M2-type macrophages through IL-4Ra-mediated signaling. The genotype of *Il4ra*$^{-/-}$ mice was confirmed by blunted gene expression of *Il4ra* in both vehicle-treated and IL-4-treated *Il4ra*$^{-/-}$ mice (**Fig. 4i**).

Consistent with our *in vitro* data demonstrating no effect of IL-4 on the phosphorylation of HSL (p-HSL) in iWAT and BAT primary cells (**Fig. 3h**,**i** and **Supplementary Fig. 4**), we found no difference in p-HSL in mice chronically treated with IL-4 relative to controls (**Fig. 4j**–**n**). Supporting these data, HPLC analysis revealed no difference in the levels of catecholamines, including NE or their metabolites, in cold-exposed mice treated chronically with IL-4 (**Fig. 4o**).

We next evaluated the metabolic effect of chronic IL-4 treatment in C57BL/6 WT and *Ucp1*$^{-/-}$ mice housed at thermoneutrality (30 °C) to assess a possible role of UCP1 in driving the reported effects of IL-4 on energy homeostasis. We administered IL-4 (50 µg/kg) daily for 8 d, and after the final injection, we recorded energy expenditure at 30 °C and during a gradual decrease of the ambient temperature to 10 °C. Chronic treatment with IL-4 had no effect on body weight (**Fig. 5a**) or body composition (**Fig. 5b**,**c**), as compared to vehicle controls. Measurement of resting metabolic rate revealed no differential effect caused by IL-4 at any tested temperature, and we observed no difference between WT and *Ucp1*$^{-/-}$ mice (**Fig. 5d**,**e**). Of note, insulation, defined as the inverse of the slope of the Scholander plot at

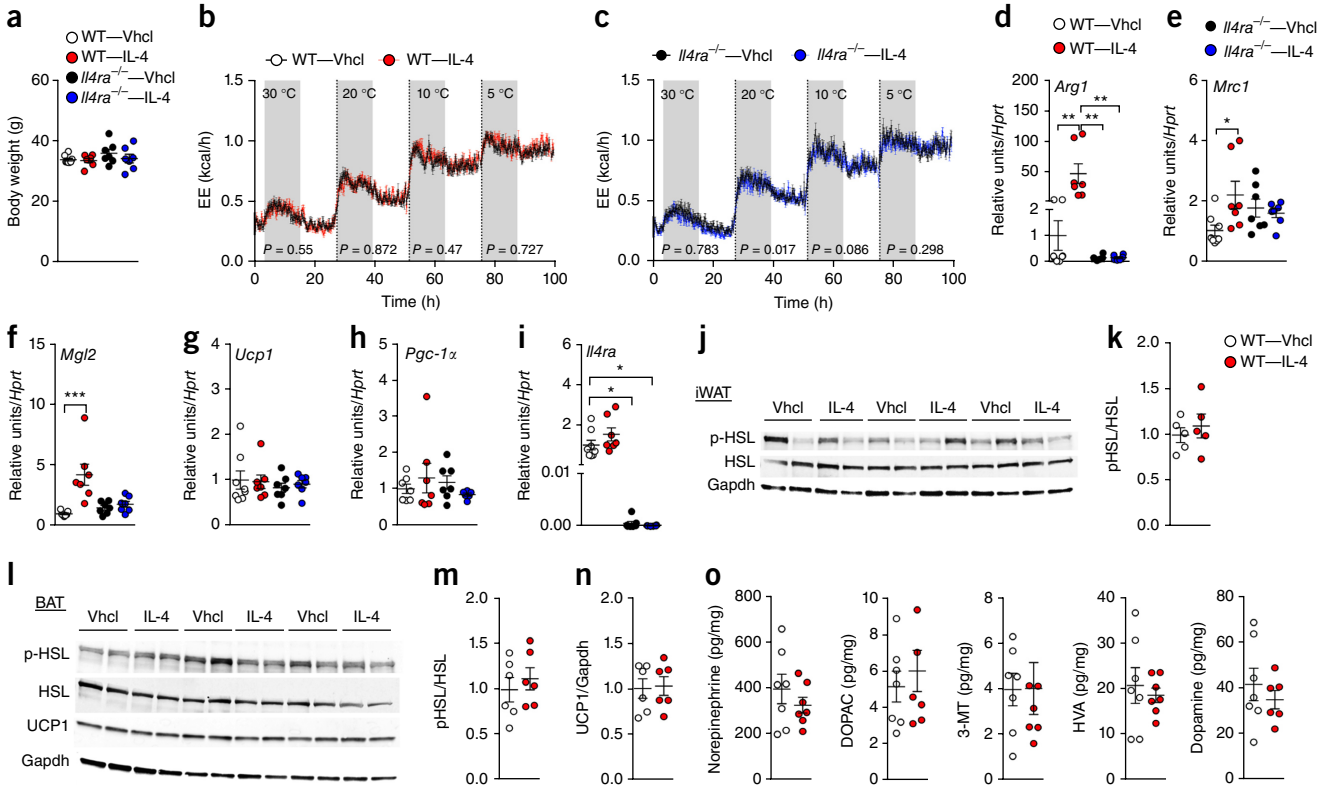

Figure 4 Effect of IL-4 on energy expenditure and thermogenesis in WT and *Il4ra*$^{-/-}$ mice at different temperatures. (**a**–**c**) Body weight (**a**) and energy expenditure of saline (Vhcl) or IL-4 (50 µg/kg)-treated WT ($n = 8$ and $n = 7$) (**b**) or *Il4ra*$^{-/-}$ mice ($n = 7$ each treatment) (**c**) was recorded over 4 d with ambient temperature decreasing from 30 °C to 20 °C to 10 °C to 5 °C (24-h measurement for each temperature). (**d**–**i**) Gene expression of M2-macrophage markers *Arg1* (**d**), *Mrc1* (**e**), *Mgl2* (**f**), brown-fat-specific markers *Ucp1* (**g**), *Pgc-1α* (**h**) and IL-4Ra, *Il4ra* (**i**), normalized to the housekeeping gene *Hprt*, of BAT from cold-exposed WT or *Il4ra*$^{-/-}$ mice treated with either vehicle ($n = 7$ or 8 and $n = 6$ or 7) or IL-4 ($n = 6$ or 7 in each treatment); each dot represents one animal. (**j**–**n**) Protein analysis of iWAT (**j**,**k**) and BAT (**l**–**n**) from cold-exposed WT mice treated with either vehicle ($n = 6$) or IL-4 ($n = 6$). Uncropped western blot images are shown in **Supplementary Figure 11**. Catecholamines and metabolites (norepinephrine, 3,4-dihydroxyphenylacetic acid (DOPAC), 3-methoxytyramine (3-MT), homovanillic acid (HVA) and dopamine) were measured in BAT from cold-exposed mice treated with vehicle ($n = 7$) or IL-4 ($n = 7$) (**o**). Data represent means ± s.e.m. $^{*}P < 0.05$; $^{**}P < 0.01$; $^{***}P < 0.001$ on the basis of one-way ANOVA followed by Bonferroni multiple-comparison test (**a**,**d**–**i**), analysis of covariance (ANCOVA) with body weight and body composition (fat and lean tissue mass) as covariate (**b**,**c**) or two-sided Student's *t*-test (**k**,**m**–**o**).

sub-thermoneutral conditions, also revealed no effect of IL-4 in thermal conductance in either WT or *Ucp1*$^{-/-}$ mice (**Fig. 5f**). IL-4 treatment induced *Arg1* expression in the BAT of cold-exposed mice lacking *Ucp1* relative to control, which again confirms successful M2 polarization by IL-4 (**Fig. 5g**). We further assessed BAT *Ucp1* mRNA and protein levels to confirm the genotype of the *Ucp1*$^{-/-}$ and WT mice (**Fig. 5h**,**i**). Notably, the amounts of UCP1 protein in BAT remained unaffected by IL-4 treatment of WT mice (**Fig. 5i**). Taken together, these data strongly imply that alternatively activated macrophages do not directly regulate thermogenesis *in vitro* or *in vivo*.

Macrophages do not express *Th* or synthesize catecholamines

To assess the ability of macrophages to synthesize catecholamines, we studied *Th* expression in a reporter mouse expressing tdTomato under control of the *Th* promoter (*Th*^{cre}:r26-tdTomato). FACS analysis readily revealed tdTomato-labeled CD11b^{+} CD14^{+} F4/80^{+} cells, which represent macrophages, in Pan-r26-tdTomato control mice, which served as positive controls (**Fig. 6a**). However, we detected no tdTomato signal in BAT macrophages of *Th*^{cre}:r26-tdTomato reporter mice maintained at room temperature or after exposure of mice to 4 °C for 8 h (**Fig. 6a**). This is consistent with the observation that a peripheral-hematopoietic-cell-specific *Th* deletion does not affect energy expenditure (**Fig. 2c**,**d**). Furthermore, we also detected no double-positive cells in histological analysis following TH staining of BAT sections of *Rosa26*-stop-GFP mutant mice crossed with mice expressing Cre under the direction of the *Cx3cr1* promoter (*Cx3cr1*^{cre}:r26-YFP mice) (**Fig. 6b**) or following two-photon microscopy of *Cx3cr1*-GFP:*Th*^{cre}:r26-tdTomato double-reporter mice (**Fig. 6c**). Finally, and corroborating the inability of macrophages to produce TH, RNA sequencing of macrophage populations isolated from various tissues, including BAT, revealed no *Th* transcripts in any of the tested macrophage populations (**Fig. 6d**). Assessment of *Th* expression in iWAT similarly revealed no mRNA expression of *Th* (**Supplementary Fig. 7**). Besides, we detected no colocalization of TH and Mac-2 signal in the iWAT or BAT of WT mice kept at either room temperature or cold exposure (5 °C) (**Supplementary Fig. 8a**,**b**). Of note, in BAT, we were able to detect only a very low number of Mac-2-positive macrophages (**Supplementary Fig. 8b**,**c**).

We further evaluated a previously proposed role of adiponectin in M2 polarization and thermogenesis in subcutaneous iWAT[9]. We found that protein concentrations of adiponectin are lower, rather than higher, in cold-acclimated mice (exposed to 4 °C for 4–5 weeks) relative to mice maintained at thermoneutrality, whereas adiponectin (*Adipoq*) mRNA levels remained unchanged (**Supplementary Fig. 9**).

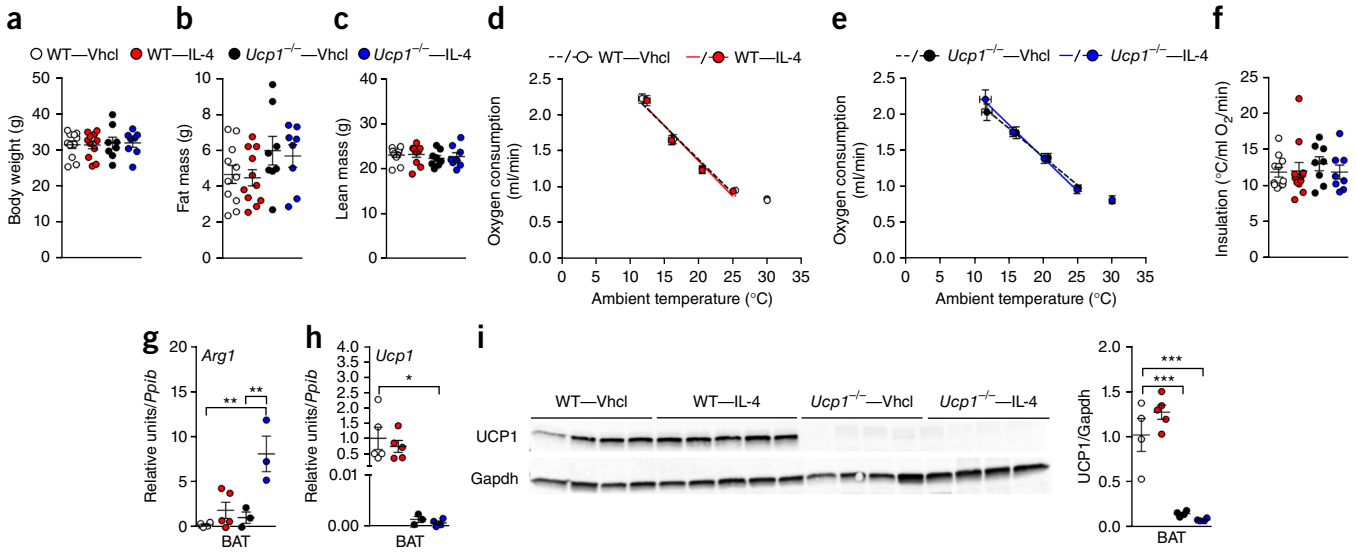

Figure 5 Effect of IL-4 on thermogenesis in WT and *Ucp1*$^{-/-}$ mice. (**a**–**c**) Body weight (**a**) and body composition (**b**,**c**) of saline (Vhcl) or IL-4 (50 µg/kg)-treated WT and *Ucp1*$^{-/-}$ mice. (**d**–**f**) Scholander plot of Vhcl-treated ($n = 11$) or IL-4-treated ($n = 11$) WT (**d**) or *Ucp1*$^{-/-}$ ($n = 8$ each treatment) (**e**) mice and calculated insulation of all groups (**f**). (**g**–**i**) Gene expression of *Arg1* (**g**) and *Ucp1* (**h**), normalized to the housekeeping gene *Ppib*, ($n = 4$ or 5 WT and $n = 3$ or 4 *Ucp1*$^{-/-}$ each treatment; each dot represents one animal), as well as protein levels of UCP1 (**i**) from BAT of WT and *Ucp1*$^{-/-}$ mice treated with Vhcl ($n = 4$ WT and $n = 4$ *Ucp1*$^{-/-}$) or IL-4 ($n = 5$ WT and $n = 4$ *Ucp1*$^{-/-}$). Uncropped western blot images are shown in **Supplementary Figure 12**. Data represent means ± s.e.m. $^{*}P < 0.05$; $^{**}P < 0.01$; $^{***}P < 0.001$ on the basis of a one-way ANOVA followed by Bonferroni multiple-comparison test.

The exposure of WT mice to 4 °C for 6 h led to higher mRNA levels of *Ucp1* and *Pgc-1α* (**Supplementary Fig. 10a**,**b**), but notably lower expression of markers indicative of M1 and M2 polarization (**Supplementary Fig. 10c**,**d**), which suggests that macrophage density is reduced during cold-induced sympathetic stimulation of iWAT. HPLC analysis of catecholamines revealed higher absolute levels of dopamine, 3,4-dihydroxyphenylacetic acid, 3-methoxytyramine and homovanillic acid in BAT of cold-exposed mice relative to mice held at room temperature (22 °C) (**Supplementary Fig. 10e**–**h**). BAT levels of NE and epinephrine are reduced in the cold-exposed mice relative

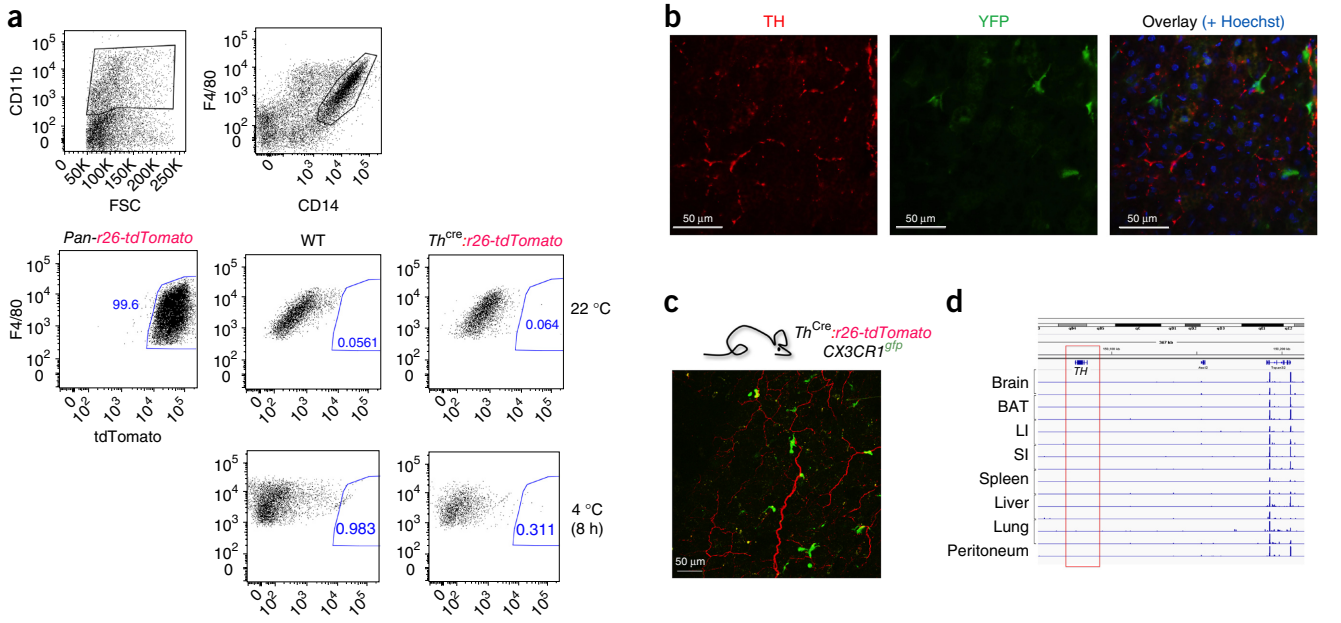

Figure 6 TH staining of BAT macrophages. (**a**) Representative FACS analysis of BAT macrophages isolated from Pan-r26-tdTomato, WT and *Th*^{cre}:r26-tdTomato mice ($n = 2$ each genotype), either from mice housed at 22 °C or at 4 °C for 8 h; (top) macrophage gating strategy on CD11b-, F4/80- and CD14-expressing cells. (**b**) Representative histology of BAT taken from *Cx3cr1*^{cre}:r26-YFP animals in 22 °C, stained for TH (red) and YFP (green) ($n = 2$). Scale bars, 50 µm. (**c**) Representative two-photon live imaging of BAT taken from *Cx3cr1*-GFP:*Th*^{cre}:r26-tdTomato mice at 22 °C ($n = 5$). Scale bar, 50 µm. (**d**) Integrative Genomics Viewer (IGV) plots of RNA-sequencing data of the *Th* locus of macrophages isolated from brain, BAT, spleen, liver, peritoneum, large and small intestine (LI, SI) under steady state; data are from ref. 21, except for BAT macrophages (S.J., unpublished data). Displayed results in **d** were performed in technical duplicates.

to room temperature controls, which likely reflects enhanced NE turnover during cold stimulation (**Supplementary Fig. 10i,j**).

In summary, these data demonstrate that peripheral, hematopoietic-cell-specific *Th* deficiency does not affect energy expenditure, and that macrophages lack the capacity to produce sufficient amounts of catecholamines to promote thermogenic effects in iWAT or BAT.

DISCUSSION

Thermogenesis is crucial for the survival of homeotherms and plays a key part in energy homeostasis. There is solid evidence indicating that thermogenesis is regulated via the sympathetic nervous system through the release of NE, and that consequent activation of β-adrenergic receptors induces lipolysis and drives BAT thermogenesis[10,11]. Given the therapeutic potential of targeting thermogenesis to improve metabolic diseases, it is of high biological and clinical relevance to determine whether there are alternative mechanisms that regulate WAT lipolysis and BAT thermogenesis. Hence, it is important to examine whether catecholamines are produced by sources other than the SNS and/or the adrenal gland, because that could lead to the identification of targetable pathways for the development of novel therapeutics. Recent studies have suggested that M2 macrophages represent one such alternative source of catecholamines. Specifically, it was reported that M2 macrophages synthesize NE *de novo*, and in a paracrine fashion, locally activate β-adrenergic-receptor signaling in nearby WAT and BAT adipocytes to induce lipolysis and BAT thermogenesis[6,7]. Furthermore, meteorin-like, a circulating hormone secreted from adipose tissue upon cold exposure, has recently been proposed to potentially promote nonshivering thermogenesis through enhanced recruitment of M2-type macrophages[12]. Similarly, it has been suggested that adiponectin induces browning of subcutaneous WAT by triggering M2-macrophage proliferation upon cold stimulation[9]. Recently, another immune cell type, type-2 innate lymphoid cells (ILC2s), has been reported to elicit the activation of alternative macrophages through IL-4-receptor signaling and to have a role in the regulation of beige/brite fat biogenesis[13]. Moreover, caloric restriction has recently been shown to promote browning of WAT through type-2 cytokine signaling[14], although caloric restriction did not affect the levels of ILC2s in those studies. Of note, it has been shown that IL-33-elicited ILC2s promote 'beiging' independently of eosinophils or the IL-4Ra signaling pathway[15].

If alternatively activated macrophages are indeed an important source of catecholamines through *de novo* synthesis of catecholamines to induce WAT lipolysis, subcutaneous WAT browning and BAT thermogenesis, then one would predict that the elimination of catecholamine production in hematopoietic cells should impair all three processes. To test this hypothesis, we generated a mouse model that allows for inducible deletion of *Th* in all peripheral tissues, including the bone marrow, and we performed a bone marrow transplant on WT mice. Upon acceptance of the BM transplant more than 90% of macrophages were donor-derived. Notably, irradiation before the bone marrow transplantation also ablates tissue macrophages[16,17]. After we induced the *Th* deletion, specifically in hematopoietic cells, we did not observe any alteration in thermogenesis, energy expenditure or browning of subcutaneous WAT in THΔper chimeric mice and their WT controls. We also studied the direct effects of alternatively activated macrophages on the thermogenic program of adipocytes *in vitro* and observed no relevant effect of M2 macrophages on white and brown adipocyte function.

Our studies also investigated a role of alternatively activated macrophages in cold-triggered brown-fat function and thermogenesis in multiple *in vivo* and *in vitro* systems. Collectively, these studies indicate that IL-4-mediated polarization to M2 macrophages does not affect energy expenditure or thermogenesis in the iWAT and BAT of WT, $Il4ra^{-/-}$ or $Ucp1^{-/-}$ mice exposed to different ambient temperatures. Furthermore, these studies failed to detect TH expression in CX3CR1-positive mononuclear phagocytes, as revealed by flow cytometry and RNA-sequencing analysis, even after cold exposure. Absolute levels of NE, as well as of other intermediates or products of catecholamine synthesis, remained unchanged in IL-4-activated M2 macrophages or in supernatant from IL-4-stimulated BMDMs. In keeping with the lack of TH expression and NE production in macrophages, the inducible deletion of *Th* in bone marrow chimeras failed to demonstrate any impairment in energy metabolism, even upon cold exposure. Given that previous studies have argued for a role of M2 macrophages in thermogenesis and browning of iWAT[6,7,9], the source for the discrepant results remains elusive. For instance, the divergent findings could arise from differences in the composition of the gut microbiome in the mice used here relative to those in the original reports, or they could be due to different animal-housing conditions between institutions. Such seemingly insignificant factors have been shown to influence metabolic phenotypes in mouse colonies from different facilities[18]. However, given that we used several mouse models and different background strains and performed these studies at several institutions on multiple continents, this scenario is unlikely. Although previous studies have reported that macrophages release NE into the culture media *in vitro*[19], it is important to note that the serum used in cell culture contains NE. It is also of interest that non-neuronal cells, such as osteoblasts, express the norepinephrine transporter (NET), exhibit specific NE-uptake activity through NET and can catabolize, but not generate, NE[20]. Hence, macrophages, similarly to neurons, might be able to take up and release catecholamines, a process that might be regulated by IL-4 signaling.

In summary, the studies presented herein from six independent laboratories repeatedly and consistently demonstrate that alternatively activated macrophages do not relevantly affect adipocyte metabolism and adaptive thermogenesis by catecholamine production. Instead, we reconfirm the essential and pivotal role of sympathetic activation in the regulation of adipose tissue lipolysis and thermogenesis.

METHODS

Methods, including statements of data availability and any associated accession codes and references, are available in the online version of the paper.

Note: Any Supplementary Information and Source Data files are available in the online version of the paper.

ACKNOWLEDGMENTS

We thank A. Fedl, L. Sehrer, L. Müller, S. Jall, D. Heine, T. Stankiewicz, K. Gaul and A. Stanley for assistance with *in vitro* and *ex vivo* analysis. The mice with floxed *Th* were kindly provided by R. Palmiter. This work was supported in part by funding to M.H.T. from the Alexander von Humboldt Foundation, the Helmholtz Alliance *ICEMED* & the Helmholtz Initiative on Personalized Medicine *iMed* by Helmholtz Association, and the Helmholtz cross-program topic "Metabolic Dysfunction." This work was further supported by grants from the German Research Foundation DFG-TS226/1-1, DFG-TS226/3-1, SFB1123, *Nutripathos* Project ANR-15-CE14-0030, European Research Council ERC AdG *HypoFlam* no. 695054 (to M.H.T.); DFG He3260/8-1, the EU FP7 Network "DIABAT," the EU ITN Network "TRAIN" 721531 (to S.H.); NIH R01 AA023416, DK082724 and a career-development award from the American Diabetes Association (to C.B.); NIH R01DK099222 (to S.D.); NIH DK17844 (to S.C.W.); the Israeli Science Foundation and European Research Council (AdvERC grant 340345) (to S.J.) and the Swedish Research Council and the Knut and Alice Wallenberg Foundation (to J.N. and B.C.). We would like to dedicate this

manuscript to the memory of Tim Bartness, whose work delineates the important role of the SNS in adipose tissue function.

AUTHOR CONTRIBUTIONS

K.F. co-conceptualized the project, designed and performed *in vitro*, *in vivo* and *ex vivo* experiments, analyzed and interpreted data and wrote the manuscript. B.F. and C.C. helped to design experiments and interpreted data. H.H.R., K.J., D.J.O., V.v.d.H., A.C.S. and D.H. performed, analyzed and interpreted the inducible THΔper mouse, validation of antibodies and BM chimera data. A.V.K. and N.P. performed, analyzed and interpreted *in vivo* experiments in *Ucp1*$^{-/-}$ mice. J.N. and K.-W.S. performed, analyzed and interpreted catecholamine data. Y.W. and S.J. performed, analyzed and interpreted tyrosine hydroxylase staining. F.B. generated the *Il4ra*$^{-/-}$ mouse. S.D., E.G., S.K., M.J., D.M., G.C., S.H., J.N. and B.C. helped to design experiments and interpreted data. S.C.W. helped with the interpretation of data and drafting the manuscript. M.H.T. co-conceptualized the project and interpreted all data. T.D.M. and C.B. co-conceptualized the project, interpreted all data, supervised the studies and wrote the manuscript.

COMPETING FINANCIAL INTERESTS

The authors declare no competing financial interests.

1. Jastroch, M. *et al.* Seasonal control of mammalian energy balance: recent advances in the understanding of daily torpor and hibernation. *J. Neuroendocrinol.* **28** (2016).
2. Cannon, B. & Nedergaard, J. Brown adipose tissue: function and physiological significance. *Physiol. Rev.* **84**, 277–359 (2004).
3. Oelkrug, R., Polymeropoulos, E.T. & Jastroch, M. Brown adipose tissue: physiological function and evolutionary significance. *J. Comp. Physiol. B* **185**, 587–606 (2015).
4. Cypess, A.M. & Kahn, C.R. Brown fat as a therapy for obesity and diabetes. *Curr. Opin. Endocrinol. Diabetes Obes.* **17**, 143–149 (2010).
5. Bartelt, A. *et al.* Brown adipose tissue activity controls triglyceride clearance. *Nat. Med.* **17**, 200–205 (2011).
6. Nguyen, K.D. *et al.* Alternatively activated macrophages produce catecholamines to sustain adaptive thermogenesis. *Nature* **480**, 104–108 (2011).
7. Qiu, Y. *et al.* Eosinophils and type 2 cytokine signaling in macrophages orchestrate development of functional beige fat. *Cell* **157**, 1292–1308 (2014).
8. Thomas, S.A., Matsumoto, A.M. & Palmiter, R.D. Noradrenaline is essential for mouse fetal development. *Nature* **374**, 643–646 (1995).
9. Hui, X. *et al.* Adiponectin enhances cold-induced browning of subcutaneous adipose tissue via promoting M2 macrophage proliferation. *Cell Metab.* **22**, 279–290 (2015).
10. Hsieh, A.C. & Carlson, L.D. Role of adrenaline and noradrenaline in chemical regulation of heat production. *Am. J. Physiol.* **190**, 243–246 (1957).
11. Bartness, T.J., Vaughan, C.H. & Song, C.K. Sympathetic and sensory innervation of brown adipose tissue. *Int. J. Obes.* **34** (Suppl. 1), S36–S42 (2010).
12. Rao, R.R. *et al.* Meteorin-like is a hormone that regulates immune-adipose interactions to increase beige fat thermogenesis. *Cell* **157**, 1279–1291 (2014).
13. Lee, M.W. *et al.* Activated type 2 innate lymphoid cells regulate beige fat biogenesis. *Cell* **160**, 74–87 (2015).
14. Fabbiano, S. *et al.* Caloric restriction leads to browning of white adipose tissue through type 2 immune signaling. *Cell Metab.* **24**, 434–446 (2016).
15. Brestoff, J.R. *et al.* Group 2 innate lymphoid cells promote beiging of white adipose tissue and limit obesity. *Nature* **519**, 242–246 (2015).
16. Merad, M. *et al.* Langerhans cells renew in the skin throughout life under steady-state conditions. *Nat. Immunol.* **3**, 1135–1141 (2002).
17. Ginhoux, F. *et al.* Fate mapping analysis reveals that adult microglia derive from primitive macrophages. *Science* **330**, 841–845 (2010).
18. Ussar, S., Fujisaka, S. & Kahn, C.R. Interactions between host genetics and gut microbiome in diabetes and metabolic syndrome. *Mol. Metab.* **5**, 795–803 (2016).
19. Flierl, M.A. *et al.* Phagocyte-derived catecholamines enhance acute inflammatory injury. *Nature* **449**, 721–725 (2007).
20. Ma, Y. *et al.* Extracellular norepinephrine clearance by the norepinephrine transporter is required for skeletal homeostasis. *J. Biol. Chem.* **288**, 30105–30113 (2013).
21. Lavin, Y. *et al.* Tissue-resident macrophage enhancer landscapes are shaped by the local microenvironment. *Cell* **159**, 1312–1326 (2014).

ONLINE METHODS

General experimental approaches for *in vivo* experiments. For *in vivo* studies, group sizes of seven or eight mice were preferentially used, which was determined from previous experiments as optimal for *in vivo* evaluation. Smaller group sizes were used in the studies involving genetically or chemically modified animals, in case there were not sufficient numbers available to reach the preferred group size of seven or eight.

For measurements of IL-4 induction of energy expenditure, group-size estimations were based upon a power calculation to minimally yield an 80% chance of detecting a 20% difference in energy expenditure between the treatment groups, and under the assumption of an alpha level of 0.05 and a s.d. of 13% in both groups.

For *in vivo* studies, mice were randomized into the treatment groups on the basis of body weight and body composition (fat and lean tissue mass). For *in vivo* experiments, all mice except the ones used in the $Ucp1^{-/-}$ study were on a C57BL/6J background. $Ucp1^{-/-}$ and WT mice were on a C57BL/6 background. All mice were maintained under specific-pathogen-free (SPF) conditions. Experiments were performed nonblinded. We screened for singular, statistically significant outliers using the maximum normal residual (Grubb's) test, but no outliers were detected for *in vivo* experiments.

Mice. All animal procedures were approved by either the Mount Sinai School of Medicine, Institutional Animal Care and Use Committee (IACUC) protocols, CCHMC IACUC, the Weizmann Institute Animal Care Committee, the Animal Ethics Committee of the North Stockholm region or the regional animal-welfare committee of the state of Bavaria.

We generated inducible peripheral *Th*-knockout mice by crossing $Th^{flox/flox}$ mice (kindly provided by R. Palmiter, University of Washington) with tamoxifen-inducible $Rosa26^{CreERT2}$ mice (Taconic #6466, Hudson, NY). The resultant $Th^{flox/flox}$;$Rosa26^{CreERT2+/-}$ mice (THΔper mice) and the $Th^{flox/flox}$;$Rosa26^{CreERT2-/-}$ (WT littermates) expressed normal levels of TH protein during development and before tamoxifen induction of the KO. Deletion of the *Th* gene was achieved by tamoxifen administration and was limited to the periphery, owing to low expression of Cre recombinase in the CNS[22]. Here we used male 28-week-old WT or THΔper mice ($n = 4$ each genotype).

To generate mice with inducible *Th* deficiency (THΔper chimera) restricted to hematopoietic cells, we injected 4×10^6 T cell–depleted BM cells from non-induced THΔper ($CD45.2^+$) ($n = 2$ males and $n = 3$ females, age of 14 weeks) or WT ($CD45.1^+$) ($n = 2$ males and $n = 3$ females, age of 4–8 weeks) mice intravenously (i.v.) into lethally irradiated (2×600 rads) $CD45.1^+$ congenic (B6.SJL-$Ptprc^a$ $Pepc^b$/BoyJ; #002014; the Jackson Laboratory, USA) ($n = 2$ males and $n = 3$ females, age of 4–8 weeks) or WT ($CD45.2^+$) ($n = 2$ males and $n = 3$ females, age of 19–22 weeks at injection) mice, as described[23]. We assessed reconstitution of the immune system ~8 weeks later by differentiating donor-derived ($CD45.2^+$) and host-derived cell populations in peripheral blood, according to CD45.1/CD45.2 expression patterns, and we used mice with a donor reconstitution of >90% for all subsequent experiments.

We used the following mouse strains to generate reporter mice: $Cx3cr1^{gfp/+}$ mice (JAX stock 005582 B6.129P-Cx3cr1tm1Litt/J, $Cx3cr1^{Cre}$(JAX stock 025524 B6J.B6N(Cg)-Cx3cr1tm1.1(cre)Jung/J); *tdTomato* reporter mice (JAX stock 007908 B6.129S6-Gt(ROSA)26Sor<tm14(CAG-tdTomato)Hze>/J) and Th^{Cre} mice (male 8-week-old mice).

Analysis of mouse metabolic phenotypes. We analyzed body composition (fat and lean mass) using a magnetic-resonance whole-body composition analyzer (EchoMRI, Houston, TX). We assessed energy intake, energy expenditure and home-cage activity by usage of an indirect calorimetric system (TSE PhenoMaster, TSE Systems, Bad Homburg, Germany). Data for energy expenditure were analyzed using analysis of covariance (ANCOVA) with body weight and body composition (fat and lean tissue mass) as covariates, as previously described[24].

IL-4 pharmacology studies. To assess the effect of IL-4 on energy expenditure, we treated male C57BL/6J and $Il4ra^{-/-}$ mice (4 months of age) daily for 12 consecutive days through intraperitoneal administration of either vehicle (0.9% saline, Braun, Melsungen, Germany) or recombinant IL-4 (50 μg/kg; Peprotech, Rocky Hill, NJ). Mice were acclimated to the metabolic chambers for 24 h before start of the measurement. Prior to study-day 9, mice were kept at thermoneutrality (30 °C) and then housed for 24 h at 20 °C followed by 24 h at 10 °C and 24 h at 5 °C. We then killed mice for subsequent tissue analysis and catecholamine quantification.

We back-crossed mice lacking UCP1 ($Ucp1^{-/-}$) (progeny of those described in ref. 25) to C57BL/6 for more than ten generations, and after intercrossing, mice lacking UCP1 ($Ucp1^{-/-}$) were maintained in parallel with the WT C57BL/6 mice. They were fed *ad libitum* (R70 Standard Diet, Lactamin), had free access to water, and were kept at a 12 h:12 h light–dark cycle at the normal (22 °C) vivarium temperature. To determine the effects of IL-4 on energy expenditure, male WT and $Ucp1^{-/-}$ mice were acclimated to 30 °C at least 4 weeks before the experiment. We treated 4-month-old mice daily (at 11:00 h) for 8 consecutive days through intraperitoneal administration of either vehicle (0.9% saline) or recombinant IL-4 (50 μg/kg; Peprotech, Rocky Hill, NJ) at 30 °C. On day 9, mice were placed into indirect-calorimetry metabolic chambers (INCA, Somedic, Horby, Schweden) with free access to food and water. After overnight acclimation at 30 °C, the temperature in the chambers was gradually decreased to 10 °C (2–3 h at each temperature). After the experiment, mice were kept at 30 °C for 3 weeks for recovery from the treatment. After recovery, mice were inversely assigned to the control and treated groups (former control mice became treated and vice versa), and the experiment was repeated. Mice were finally killed after energy expenditure was recorded. Time between last injection of IL-4 and euthanization of the mice was 48 h. At every ambient temperature, resting metabolic rate was calculated as minimal stable (during at least 10 min) oxygen consumption and was plotted versus the ambient temperature ('Scholander plots')[26]. Using total energy expenditure calculated during the last h at each temperature by means of a modified Weir equation yielded similar results[27]. The slopes of the Scholander plots at and below 26–27 °C were calculated individually for every mouse, using the best linear fit. Insulation was calculated as the inverse of the slope. Two rounds of the experiment yielded similar results.

Western blot. For the THΔper and chimera studies, we homogenized the tissues in 20-mM MOPS containing 2-mM EGTA, 5-mM EDTA, 30-mM sodium fluoride, 40-mM β-glycerophosphate, 10-mM sodium pyrophosphate, 2-mM sodium orthovanadate, 0.5% NP-40 and complete protease-inhibitor cocktail (Roche, Nutley, NJ) and centrifuged at 13,000*g* for 20 min at −4 °C. The supernatant was then collected, and protein concentration was measured using a bicinchoninic acid (BCA) protein quantification kit (Thermo Scientific, Waltham, MA). Protein extracts were separated on 4–12% NuPAGE gels (Invitrogen, Carlsbad, CA) and blotted onto Immobilon FL PVDF membranes (Millipore, Billerica, MA). Membranes were blocked at room temperature for 1 h with Odyssey LI-COR blocking buffer (LI-COR, Lincoln, NE) diluted 1:1 in Tris-buffered saline (TBS). Membranes were then incubated with primary antibodies (diluted 1:1,000 in a 1:1 blocking buffer/TBS-T solution) overnight at 4 °C. Primary antibodies against tyrosine hydroxylase (EMD Millipore, Billerica MA-MAB318, 1:1,000 dilution) and Gapdh (Santa Cruz Biotechnology, Dallas, TX-32233, 1:2,000 dilution) were used. Membranes were washed consecutively three times for 5 min each in TBS-T (0.1%). Blots were incubated with Dylight 680-conjugated goat anti–rabbit IgG and Dylight 800-conjugated goat anti–mouse IgG (Thermo Scientific, Waltham, MA) for 1 h at room temperature in blocking buffer containing 0.1% TBS-T and 0.1% SDS. Blots were washed three more times in TBS-T followed by a final wash in TBS, and the blots were then scanned with the LI-COR Odyssey (LI-COR, Lincoln, NE) and quantified with Odyssey 3.0 software on the basis of a direct fluorescence measurement. Other fat tissues were lysed in ice-cold RIPA buffer (Sigma-Aldrich, Munich, Germany) containing 1-mM PMSF (Carl Roth), 10-nM calyculin A (Cell signaling) and protease/phosphatase inhibitor (Thermo Fisher Scientific, Erlangen, Germany) using a polytron. Lysates were chilled on ice for 20 min and centrifuged for 15 min, 10,000*g*, at 4 °C. The supernatant was collected and protein concentration was as described above. Proteins were separated on a Criterion gel (Bio-Rad, Munich, Germany) and transferred on to nitrocellulose membranes. Membranes were incubated with primary antibody (Cell Signaling Technology, Danvers, MA) overnight at 4 °C, and HRP-coupled secondary antibody (Santa Cruz Biotechnology, Dallas, TX) was used to detect protein signal through the LI-COR imaging system. Antibodies were purchased from Cell Signaling (Phospho-HSL (Ser660) #4126, HSL #4107, each diluted 1:2,000), Santa Cruz (Gapdh G-9, #365062, diluted 1:10,000) and Abcam (Ucp1, #23841, diluted 1:2,000).

Flow cytometry. We performed FACS analysis of BM chimera using CD45.1 and CD45.2 antibodies (BioLegend). Acquisition was performed with a BDBioscienes FACSCalibur and analysis with FlowJo software. For FACS analysis of BAT of the *CX3CR1*-GFP:*Th*^{cre}:r26-tdTomato mice, tissue was collected, dissected by scissors and then incubated for 30 min with DMEM medium (Beit Ha'emek, Israel) containing 1 mg/ml collagenase-2 (Sigma-Aldrich), 2% BSA (Sigma-Aldrich) and 12.5-mM HEPES buffer (Beit-Ha'emek, Israel). The resulting cell suspension was filtered through a 70-µm mesh, and erythrocytes were removed by ACK lysis. After cell suspension, cells were incubated in FACS buffer (PBS with 1% BSA, 2 mM EDTA and 0.05% sodium azide) in the presence of staining antibody. Antibodies used for staining were CD45 (clone 30F11, BioLegend), CD14 (clone Sa2-8, BioLegend) and F4/80 (clone BM8, Serotech).

Preparation of RNA and gene-expression analysis. Total RNA was prepared using RNeasy Kit (Qiagen, Hilden, Germany) according to the manufacturer's instructions. cDNA synthesis was performed with QuantiTect Reverse Transcription Kit (Qiagen, Hilden, Germany) according to the manufacturer's instructions. Gene expression of cell samples (n = 3 per group) was profiled with quantitative PCR-based (qPCR-based) techniques using SYBR green or TaqMan Single Probes (Thermo Fisher Scientific, Erlangen, Germany). The relative expression of the selected genes was measured using the 7900HT Fast Real-Time PCR System (Thermo Fisher Scientific, Erlangen, Germany). The relative expression levels of each gene were normalized to the housekeeping gene peptidylprolyl isomerase B (*Ppib*), hypoxanthine phosphoribosyltransferase (*Hprt*) or TATA-box binding protein (*Tbp*). RNA expression data were quantified according to the ΔC_t method, as described[28]. Sequences of all primers are listed in **Supplementary Table 1**. TaqMan Low Density Array (Thermo Fisher Scientific, Erlangen, Germany) was performed according to instructions.

Isolation and culture of BMDMs. Bone marrow from the hind legs of 6-week-old C57BL/6J or BALB/c mice was obtained, erythrocytes were lysed with ACK buffer (151 mM NH_4Cl, 10 mM $KHCO_3$, 0.2 mM EDTA in H_2O) and the bone marrow was purified using Ficoll (GE Healthcare, Munich, Germany). Monocyte differentiation into macrophages was achieved by differentiation with DMEM medium containing 30% L929 supernatant, 20% FBS and 1% penicillin/streptomycin for 5 d. BMDM polarization toward the M2 phenotype was accomplished by treatment with IL-4 (5, 10, 20 ng/ml, Peprotech, Rocky Hill, NJ) for 24 h. BMDMs and primary adipocytes were not tested for mycoplasma contamination; however, Raw264.7 and L929 cells were negatively tested for mycoplasma infection.

Isolation of primary adipocytes. iWAT was obtained from 6–8-week-old male C57BL/6J or BALB/c mice. Fat pads were minced and digested for 40 min at 37 °C (1 mg/ml Collagenase IV (Thermo Fisher Scientific, Erlangen, Germany); 3 U/ml Dispase II (Sigma-Aldrich, Munich, Germany); 0.01-mM $CaCl_2$ in PBS). The cell suspension was filtered, centrifuged and resuspended in growth medium (DMEM/F12 1:1 plus Glutamax (Thermo Fisher Scientific, Erlangen, Germany) containing 1% pen/strep and 10% FBS. Primary white adipocytes were grown to confluence (37 °C, 10% CO_2), which was followed by the induction of differentiation using dexamethasone (1 µM), isobutylmethylxanthine (0.5 mM), rosiglitazone (1 µM) and insulin (5 µg/ml) in growth medium. After 48 h of induction, cells were maintained in culture medium containing insulin (5 µg/ml) and rosiglitazone (1 µM). On day 4 of differentiation, cells were cultured in growth medium containing insulin (5 µg/ml). To stimulate thermogenesis, cells were treated with 0.5-1 µM isoproterenol (Sigma-Aldrich, Munich, Germany) dissolved in serum-free growth medium for 6 h on day 6 of adipocyte differentiation.

Primary brown adipocytes were isolated through the same procedure, with the exception that 1 mg/ml collagenase II (Thermo Fisher Scientific, Erlangen, Germany) was used for digestion. For the differentiation of primary brown adipocytes, the induction cocktail contained dexamethasone (5 µM), isobutylmethylxanthine (0.5 mM), rosiglitazone (1 µM), indomethacine (125 µM), T3 (1 nM) and insulin (0.5 µg/ml) in growth medium. At 2-d postinduction of differentiation, cells were maintained in culture medium containing rosiglitazone (1 µM), T3 (1 nM) and insulin (0.5 µg/ml). On day 4 of differentiation, cells were cultured in growth medium containing T3 (1 nM) and insulin (0.5 µg/ml). For β-adrenergic receptor activation, primary brown adipocytes were treated with 1 µM isoproterenol (Sigma-Aldrich, Munich, Germany), dissolved in serum-free growth medium for 6 h on day 6 of adipocyte differentiation.

Catecholamine measurement. For sample preparation: 100 µl of $HClO_4$ (0.3 M) and 4 µl of internal standard (DHBA, 1 ng/µl) were added to the cell pellets. The mixture was ultra-sonicated under ice for 10 s and transferred into an Amicon Ultra 0.5 ml (3 kDa) centrifugal filter unit (Merck Millipore, Darmstadt, Germany). The samples were then centrifuged at 13,000 r.p.m. for 30 min at 1 °C. The filtrate was transferred into a measurement vial and injected into the system. The supernatant was thawed, and 200 µl were transferred into an Amicon Ultra 0.5 ml (3 kDa) centrifugal filter unit (Merck Millipore, Darmstadt, Germany). 4 µl of internal standard (DHBA, 1 ng/µl) were added, and the samples were centrifuged at 13,000 r.p.m. for 30 min at 1 °C. The filtrate was transferred into a measurement vial and injected into the system. The BAT was thawed, and 200 µl of perchloric acid (0.3 M) and 4 µl of internal standard (DHBA, 1 ng/µl) were added. The samples were homogenized by ultrasonication for 30 s on ice. For this, they had to be in a 1.5-ml Eppendorf tube because bigger tubes, with their level lower end, are not sufficient for homogenization. Afterward, the samples were centrifuged at 9,000 r.p.m. for 10 min at 1 °C. The residue was usually at the bottom of the tube, so that the supernatant could be directly transferred into a measurement vial and injected into the system. If the fat layer was on top, the solution had to be taken with a 1-ml syringe fitted with a cannula and filtered through a 0.2-µm syringe filter (Whatman, Maidstone, UK) into the sample vial and was then injected into system. Measurement of monoamines and metabolites: 20 µl were injected into an Ultimate 3000 HPLC system from Thermo Fischer, consisting of an isocratic pump, an autosampler and a coulometric Ultra Analytical Cell (6011 RS). The potential was set to 0.4 V with a data-collection rate of 25 Hz. The separation of the compounds was carried out on a C_{18}-column from Waters (Atlantis T3 100Å, 3 µm, 4.6 mm × 150 mm), with a preceding security-guard cartridge (Phenomenex, AJ0-4287). An isocratic elution with a commercially available mobile phase from RECIPE (1210, ClinRep commercial HPLC) with 5.5% (v/v) added acetonitrile and a flow rate of 0.5 ml/min was used.

Histology and two-photon imaging. For immunofluorescence, tissues fixed in 4% paraformaldehyde (PFA) overnight at 4 °C, incubated with 30% sucrose for 48 h and flash-frozen with isopentane before sectioning by cryostat. Samples were blocked with PBS containing 0.05% Tween (PBS-T), 0.3% triton and 20% normal horse serum (NHS) before incubation with PBS-T containing 0.3% triton, 2% NHS and primary antibodies in 4 °C, followed by incubation with secondary antibody in PBS at RT for 1 h and final stain with Hoechst (1:25,000). Antibodies used were anti-GFP/YFP (Abcam) and anti-TH (Millipore). For two-photon imaging, interscapular BAT was isolated from indicated animals and subjected to two-photon microscopy using an upright LSM 880 NLO combined confocal-multiphoton system, (Zeiss, Germany) with Chameleon Ultra tunable Ti:Sapphire laser, Coherent (USA) with Plan-Apochromat 20×/0.8 M27 lens. For excitation of tdTomato and GFP, the laser was tuned to 900 nm and the emission filter set was 578–638 nm and 519–561 nm, respectively. Image acquisition and further visualization was performed using ZEN Imaging software (Zeiss, Germany).

RNA isolation of BAT macrophages, library construction and analysis. RNA-seq was performed as described previously[21]. In brief, 10^4 cells were sorted into 50 µl of lysis/binding buffer (Life Technologies) and stored at −80 °C. mRNA was captured with Dynabeads oligo (dT) (Life Technologies), according to the manufacturer's guidelines. We used a derivation of MARS-seq[29] to produce expression libraries with a minimum of two replicates per population. 4 million reads per library were sequenced and aligned to the mouse reference genome (NCBI 37, mm9) using HISAT v.0.15 with default parameters. Expression levels were calculated and normalized for each sample to the total number of reads using HOMER software (http://homer.salk.edu)[30]. RNA-seq analysis focused on genes in the 25th percentile of expression with a twofold differential between at least two populations. The value of k for the K-means clustering (matlab function kmeans) was chosen by assessing the average silhouette (matlab function evalclusters; higher score means more cohesive clusters) for a range of possible values, with correlation as the distance metric.

doi:10.1038/nm.4316

Depletion of macrophages from primary iWAT. Macrophages were separated from iWAT primary cells by magnetic-immunoaffinity isolation using anti-CD11b antibodies conjugated to magnetic beads (MACS Cell Separation System; Miltenyi Biotec, Bergisch Gladbach, Germany). After iWAT isolation, CD11b-positive cells were separated using positive-selection columns (LD columns; Miltenyi Biotec, Bergisch Gladbach, Germany), according to the manufacturer's instructions. For the validation of cell separation, cell eluents were taken before and after depletion of CD11b-positive cells, as well as from the retained cell fraction, bound to the conjugated beads. Successful depletion of macrophages was confirmed by flow cytometric and qPCR analysis.

Oil Red O staining and microscopy. Cells were fixed with 4% PFA at differentiation days 0, 3 or 6. Adipocytes were stained with Oil Red O (Sigma-Aldrich, Munich, Germany) for 10 min and immediately washed with H_2O. Phase-contrast microscopy was performed before and after Oil Red O staining with a Keyence BZ-9000 microscope. For lipid quantification, Oil Red O was retrieved from the cells by 100% isopropanol and absorbance was measured at 500 nm. DAPI signal was measured to correct for cell number.

Bioenergetic analysis. Primary iWAT cells were isolated, macrophage-depleted and differentiated for 5 d on a collagen-coated XF96 well plate. On the day of the experiment (day 5), cells were washed with DMEM XF Assay medium (Seahorse Bioscience, Santa Clara, CA), supplemented with 25-mM glucose, 10-mM pyruvate and 0.3% fatty-acid-free BSA, and incubated in 180 µl of XF Assay medium in a non-CO_2 incubator at 37 °C for 1 h. All port compounds were dissolved in pure DMEM XF Assay medium without supplements, and ten-fold higher concentrated compounds were loaded into the ports of a XF Assay Cartridge. Oxygen-consumption rate (OCR) was measured using an extracellular flux analyzer (XF96, Seahorse Bioscience, Santa Clara, CA). Basal OCR was recorded for 21 min, followed by measurement of OCR after injection of isoproterenol (1 µM, 35 min), oligomycin (2 µg/ml, 21 min), carbonyl cyanide-p-trifluoromethoxyphenylhydrazone (FCCP) (1 µM, 21 min), rotenone (2.5 µM)/antimycin (2.5 µM)/2-deoxyglucose (10 mM) (28 min). For normalization, the cell plate was subsequently costained with DAPI and Nile red, and the fluorescence signal was detected to correct for cell number and differentiation.

Adipocyte treatment with conditioned media from activated macrophages. Conditioned media from 24-h polarized BMDMs or Raw264.7 cells (Sigma-Aldrich, Munich, Germany) were collected and supplemented to 6-d differentiated primary adipocytes for 6 h. Raw264.7 cells have been tested and found negative for mycoplasma contamination.

Immunofluorescence. iWAT and interscapular BAT were dissected from room temperature (23 °C) or 4-h cold-exposed (5 °C) C57BL/6J mice and subsequently fixed in 4% PFA. Fat tissues was embedded in paraffin and cut in 5-µm sections in a vibratome. After deparaffinization, sections were subjected to antigen retrieval by boiling for 20 min in citrate buffer (10-mM sodium citrate in H_2O, pH = 6) in a microwave, then left to cool at room temperature for 20 min. After washing in TBS, sections were blocked in SUMI (0,25% gelatine + 0,5% TritonX in TBS) for 1 h, then incubated overnight at 4 °C with a cocktail containing primary antibodies against TH (ab152, abcam, 1:500) and Mac-2 (CL8942AP, CedarLane Labs, 1:500) diluted in SUMI. After washing in TBS, sections were incubated with a cocktail of secondary antibodies (Alexa 488 Goat anti-rabbit, R37116+ Alexa 568 Goat anti-rat, A-11077) diluted in SUMI for 1 h at room temperature. After washing in TBS, sections were incubated with 0,1% Sudan Black B (Sigma-Aldrich, Munich, Germany) in 70% EtOH for 20 min to quench autofluorescence, and then washed with TBS + 0.02% Tween20. Sections were then counterstained for 3 min with DAPI (Thermo Fisher Scientific, 62248, 1:3,000), washed in TBS, then mounted using Elvanol mounting medium. Image stacks (5-µm thick) were collected through the *z* axis at an interval of 1 µm using a Leica SP5 scanning confocal microscope equipped with a 20× and 40× objective, and final images obtained by maximum intensity projection of the *z*-stack. Number of Mac-2-positive cells was quantified using ImageJ, for each sample ($n = 3$ or 4), and the average number of cells was calculated from at least three different 20× fields from at least two different sections.

Statistics. Statistical analyses were performed by using statistical tools implemented in GraphPad Prism (version 6). Statistical analyses were performed on data distributed in a normal pattern using a regular one-way or two-way analysis of variance (ANOVA) with Bonferroni *post hoc* multiple-comparison analysis to determine statistical significance between treatment groups. Differences with P values less than 0.05 were considered to be significant. Group-size estimations were based on a power calculation to minimally yield an 80% chance of detecting a significant difference in energy expenditure or body weight of $P < 0.05$ between the treatment groups. All results are given as mean ± s.e.m. Data on gene expression were screened for singular, statistically significant outliers using the maximum normed residual (Grubb's) test implemented in GraphPad prism.

Data availability. RNA-sequencing data have been deposited in the Gene Expression Omnibus and accession codes are available, as described[21].

22. Koch, L. *et al.* Central insulin action regulates peripheral glucose and fat metabolism in mice. *J. Clin. Invest.* **118**, 2132–2147 (2008).
23. Homann, D. *et al.* Lack of intrinsic CTLA-4 expression has minimal effect on regulation of antiviral T-cell immunity. *J. Virol.* **80**, 270–280 (2006).
24. Tschöp, M.H. *et al.* A guide to analysis of mouse energy metabolism. *Nat. Methods* **9**, 57–63 (2011).
25. Enerbäck, S. *et al.* Mice lacking mitochondrial uncoupling protein are cold-sensitive but not obese. *Nature* **387**, 90–94 (1997).
26. Scholander, P.F., Walters, V., Hock, R. & Irving, L. Body insulation of some arctic and tropical mammals and birds. *Biol. Bull.* **99**, 225–236 (1950).
27. Weir, J.B. New methods for calculating metabolic rate with special reference to protein metabolism. *J. Physiol. (Lond.)* **109**, 1–9 (1949).
28. Livak, K.J. & Schmittgen, T.D. Analysis of relative gene expression data using real-time quantitative PCR and the 2(-Delta Delta C(T)) Method. *Methods* **25**, 402–408 (2001).
29. Jaitin, D.A. *et al.* Massively parallel single-cell RNA-seq for marker-free decomposition of tissues into cell types. *Science* **343**, 776–779 (2014).
30. Heinz, S. *et al.* Simple combinations of lineage-determining transcription factors prime cis-regulatory elements required for macrophage and B cell identities. *Mol. Cell* **38**, 576–589 (2010).